NEXRES 12 (2026) 102174

Contents lists available at ScienceDirect

Next Research

journal homepage: www.elsevier.com/locate/nexres

Short Communication

Lutein as a reactive xanthophyll synthon: phytochemical transformation into polyurethane networks

Rahul D. Kamble [*,a], Shrikant V. Hese [b], Ajay N. Ambhore [c], Milind V. Gaikwad [d], Shudhodan N. Kadam [e]

[a] Amruteshwar Arts, Commerce and Science College Vinzar, Pune MS 412213, India
[b] DD.Bhoyar College Of Arts And Science Mouda Nagpur (MS) 441104, India
[c] Department of Chemistry, Vivekanand College, Kolhapur MS 416003, India
[d] Department of Chemistry, D.Y. Patil ACS, College, Pimpri, Pune MS 411018, India
[e] Dr. Ganpatrao Deshmukh Mahavidyalaya, Sangola, Dist. Solapur MS 413307, India

ARTICLE INFO

Keywords:
Lutein
Xanthophyll
Bio-based polyurethanes
Step-growth polymerization
Urethane networks

ABSTRACT

Lutein, a naturally occurring dihydroxy xanthophyll abundant in plant tissues, is widely recognized for its nutritional and antioxidant properties, yet remains underexplored as a synthetic building block. In this study, lutein isolated from *Tagetes erecta* petals was utilized as a renewable lutein-derived synthon and chemically transformed via step-growth polymerization reactions with aromatic diisocyanates to afford lutein-derived polyurethane (LPU) networks. The conversion of hydroxyl functionalities into urethane linkages was confirmed by spectroscopic analyses, demonstrating the successful incorporation of the natural pigment scaffold into LPU networks. This work highlights a sustainable strategy for extending the chemical utility of lutein beyond its conventional applications.

1. Introduction

Polyurethanes (PUs) represent one of the most versatile classes of polymeric materials owing to their excellent mechanical strength, chemical resistance, tunable elasticity, and ease of structural modification [1,2]. Since their discovery, polyurethane materials have found widespread applications in coatings, adhesives, elastomers, foams, biomedical devices, packaging materials, automotive components, textiles, and advanced functional composites [3,4]. Conventional polyurethane synthesis is primarily based on the polyaddition reaction between polyols and diisocyanates derived from petrochemical resources [5,6]. Although these materials possess outstanding performance characteristics, their dependence on non-renewable feedstocks and the environmental concerns associated with fossil-based production have stimulated extensive research toward sustainable alternatives [5–7].

Recent advances in green polymer chemistry have focused on replacing petroleum-derived polyols with renewable biomass-derived precursors [8]. A wide variety of natural resources, including vegetable oils, lignin, cellulose, starch, chitosan, natural sugars, terpenes, proteins, and plant-derived polyphenols, have been investigated as sustainable building blocks for polyurethane synthesis [9]. These bio-based materials offer several advantages, including reduced carbon footprint, lower dependence on fossil resources, potential biodegradability, and improved environmental compatibility [10]. Consequently, bio-based polyurethane systems have emerged as promising candidates for the development of environmentally benign coatings, packaging materials, biomedical scaffolds, and functional polymer networks [10,11].

The synthesis of sustainable polyurethane materials has evolved considerably during the last decade. Vegetable oil-derived polyols obtained from soybean, castor, linseed, sunflower, and palm oils have been extensively utilized owing to their availability and ease of chemical functionalization [12,13]. Similarly, lignin-based polyurethanes have attracted significant attention because of their aromatic structure, high rigidity, and abundant hydroxyl functionalities [13,14]. Cellulose, starch, and chitosan-based polyurethane materials have also been developed to improve biodegradability, mechanical performance, and biocompatibility. More recently, amino acid derived diisocyanates, non-isocyanate polyurethane (NIPU) systems, and self-healing

* Corresponding author.
E-mail address: rdkamble143@gmail.com (R.D. Kamble).

https://doi.org/10.1016/j.nexres.2026.102174
Received 16 March 2026; Received in revised form 1 July 2026; Accepted 15 July 2026
Available online 15 July 2026

polyurethane networks have been reported as environmentally safer alternatives to conventional formulations [15,16].

Despite these advances, several challenges remain associated with currently available bio-based polyurethane systems. Vegetable oil-based polyols typically contain long aliphatic chains that generate flexible soft segments, often resulting in lower glass-transition temperatures and reduced thermal resistance [17]. Lignin-derived systems frequently suffer from structural heterogeneity and processing difficulties [14,15], while polysaccharide-based materials often require extensive chemical modification to achieve adequate solubility and reactivity [18]. Furthermore, many renewable polyurethane formulations rely on multistep synthetic procedures involving oxidation, epoxidation, hydrolysis, or transesterification prior to polyurethane formation, increasing processing complexity and cost [15,17].

In parallel with developments in sustainable polymer chemistry, increasing attention has been directed toward the valorization of naturally occurring phytochemicals as renewable molecular synthons. The seventh principle of green chemistry advocates the use of renewable feedstocks for the development of sustainable materials and chemicals [1]. Plant secondary metabolites constitute a structurally diverse reservoir of renewable molecules that can be transformed into value-added materials through controlled chemical modification [19]. However, most phytochemical research continues to focus predominantly on biological activities, whereas their potential as reactive building blocks for advanced polymeric materials remains comparatively underexplored.

Carotenoids represent an important class of naturally occurring plant pigments characterized by extended π-conjugation, molecular rigidity, and unique structural functionalities. Among them, lutein is a naturally occurring dihydroxy xanthophyll abundantly present in green leafy vegetables and particularly concentrated in marigold (*Tagetes erecta*) petals. Owing to its two terminal hydroxyl groups and highly conjugated polyene backbone, lutein possesses intrinsic bifunctionality that makes it a potentially attractive renewable precursor for polyurethane synthesis [20]. Unlike conventional vegetable oil-derived polyols, which primarily contribute flexible aliphatic segments to polymer networks, lutein introduces a rigid and highly conjugated molecular framework capable of influencing molecular organization, chain packing, thermal behavior, and surface properties [20].

To date, research on lutein has focused mainly on its antioxidant, anti-inflammatory, photoprotective, cardioprotective, and anticancer activities [21–23]. Chemical modifications of lutein have largely been limited to esterification reactions aimed at improving stability, storage properties, or bioavailability [22–24]. Although carotenoid derivatives have occasionally been incorporated into polymer matrices as additives or stabilizers, the direct utilization of lutein as a reactive molecular synthon for polyurethane network formation has received little attention. Consequently, a significant knowledge gap exists regarding the ability of lutein to participate directly in step-growth polymerization reactions and influence the resulting physicochemical properties of polyurethane materials [20].

From a phytochemical perspective, transforming lutein from a biologically active pigment into a structural component of polymeric networks represents a shift from conventional structure-activity relationships toward a structure-reactivity paradigm [20,25]. Such an approach expands the functional relevance of naturally occurring metabolites beyond their traditional biological roles while creating opportunities for the development of novel renewable materials [25]. Furthermore, the direct utilization of lutein as a diol precursor eliminates the need for extensive pre-functionalization steps often required for many biomass-derived polyols, thereby providing a comparatively straightforward route toward bio-based polyurethane synthesis [20].

In the present study, lutein isolated from marigold (*Tagetes erecta*) petals was employed as a naturally occurring diol and reacted directly with aromatic diisocyanates, namely methylene diphenyl diisocyanate (MDI) and toluene diisocyanate (TDI), to generate LPU networks. The influence of NCO/OH stoichiometry on molecular weight characteristics, molecular organization, thermal stability, coating performance, and surface-related properties was systematically investigated. Compared with conventional vegetable oil-derived polyurethane systems, the present approach introduces a rigid carotenoid-based molecular architecture that combines renewable origin with structural functionality. The present work demonstrates the feasibility of utilizing lutein as a renewable xanthophyll synthon and establishes clear relationships between molecular architecture, network formation, thermal stability, coating performance, and chemical durability.

2. Materials and methods

2.1. Materials

Lutein was extracted and purified from marigold (*Tagetes erecta*) petals following a modified literature protocol [26–27]. Methylene diphenyl diisocyanate (MDI) and toluene diisocyanate (TDI) were employed as received without further purification. Dibutyltin dilaurate (DBTDL) was used as the urethane–forming catalyst. All solvents and chemicals were of analytical or synthesis grade and used without additional purification unless otherwise specified.

2.2. Extraction and purification of lutein from tagetes erecta petals

Freshly collected marigold (*Tagetes erecta*) petals were washed, shade-dried, and finely ground into a homogeneous powder. The carotenoid-rich fraction was extracted using a tetrahydrofuran (THF)/petroleum ether solvent mixture (1:1, v/v) containing 0.1 wt% butylated hydroxytoluene (BHT) to minimize oxidative degradation of lutein during processing. The resulting extract was filtered to remove insoluble plant residues and subsequently subjected to saponification with 10% (w/v) methanolic potassium hydroxide (KOH) at room temperature for 4 h. This treatment hydrolyzed naturally occurring lutein esters, yielding free lutein diol suitable for polyurethane synthesis.

Following saponification, the unsaponifiable fraction was extracted with diethyl ether and repeatedly washed with deionized water until a neutral pH was attained. The organic layer was dried over anhydrous sodium sulfate (Na_2SO_4) and concentrated under reduced pressure. The crude lutein obtained was purified by recrystallization from a hot hexane solvent system, affording bright yellow crystalline lutein. The purity of the isolated lutein was confirmed by UV–Vis spectrophotometry.

2.3. Xanthophyll-Derived polyurethane synthesis

Lutein, containing two terminal hydroxyl groups, was utilized as a bio-based diol for polyurethane synthesis. LPU networks were prepared through step-growth polyaddition reactions between lutein and methylene diphenyl diisocyanate (MDI), toluene diisocyanate (TDI), or their combination. Dibutyltin dilaurate (DBTDL, 0.5 wt% relative to lutein) was used as the catalyst, and N,N-dimethylacetamide (DMAc) served as the reaction medium.

Purified lutein was dissolved in DMAc and added dropwise to a stirred solution of the respective diisocyanate. The reactions were carried out at room temperature using NCO/OH molar ratios ranging from 0.5:1.0 to 3.0:1.0 to examine the effect of NCO/OH stoichiometry on polyurethane formation and network development. The resulting reaction mixtures were cast onto glass substrates and cured under controlled conditions to obtain LPU films.

2.3.1. Film casting and curing parameters

The homogeneous dimethylacetamide (DMAc) solution containing the lutein-transformed prepolymer mixture was systematically degassed under vacuum for 15 min to eliminate entrapped microbubbles. The solution was subsequently cast onto ultra-clean, polished steel panels and high-density polyethylene (HDPE) molds using a calibrated doctor

blade to achieve a uniform wet film thickness of approximately 100 μm. The cast films underwent a controlled thermal curing cycle: initial solvent evaporation was conducted at 40 °C for 4 h under a mild vacuum, followed by step-wise temperature ramping to 80 °C for 6 h, and a final post-curing phase at 110 °C for 2 h under an inert nitrogen atmosphere to ensure complete chemical conversion of residua l functional groups.

2.4. Characterization

2.4.1. Chemical characterization of lutein and reactive precursors

The chemical structure and purity of lutein were confirmed by Fourier-transform infrared (FTIR) spectroscopy, ^{1}H NMR spectroscopy, and mass spectrometry. The corresponding spectra are provided in the Supplementary Information (Figures S1–S3). The characteristic FTIR spectra of methylene diphenyl diisocyanate (MDI) and toluene diisocyanate (TDI) are also included in the Supplementary Information (Figures S4 and S5).

The isocyanate (NCO) content of MDI and TDI was determined by the n-butylamine back-titration method according to ASTM D2572–97. The hydroxyl value of lutein was measured by the acetylation method following the procedure prescribed by the Indian Standards Institution (ISI: 354, 1987). These analyses provided essential compositional parameters for calculating the NCO/OH stoichiometry employed in polyurethane synthesis.

2.5. Chemical transformation of lutein

Fourier transform infrared (FTIR) spectra were recorded using a Shimadzu FTIR spectrometer (Japan) over the range of 4000–500 cm^{-1} to monitor the chemical transformation of lutein during polyurethane formation. Polymer samples were prepared as KBr pellets and analyzed to identify characteristic functional group changes, with particular emphasis on the disappearance of lutein hydroxyl absorptions and the emergence of urethane-specific bands, thereby confirming successful conversion of lutein into LPU networks.

2.6. Molecular weight determination

The molecular weight characteristics of the LPU networks were determined by gel permeation chromatography (GPC) using an Agilent GPC-Addon Rev A02.02 HPLC system equipped with a PL-gel Agilent column, with tetrahydrofuran (THF) as the eluent under ambient conditions, yielding Mn, Mw, and polydispersity index (PDI) values. Intrinsic viscosity measurements were carried out at 25 °C using an Ubbelohde capillary viscometer with THF as solvent to assess the hydrodynamic volume and solution behavior of the lutein-transformed chains and to support molecular weight trends observed from GPC analysis.

2.7. Thermal behavior of LPU networks

Thermal behavior of the LPU networks was evaluated by thermogravimetric analysis (TGA) using a TA Q500 thermogravimetric analyzer, in which approximately 3 mg of sample was heated in a platinum pan under a nitrogen atmosphere (10 mL min^{-1}) from room temperature to 550 °C at a heating rate of 10 °C min^{-1}, and the corresponding mass loss was recorded as a function of temperature. Differential scanning calorimetry (DSC) was performed using a TA Instruments Q100 calorimeter (New Castle, DE, USA) to examine thermal transitions associated with the chemically transformed LPU networks.

2.8. Structure-Property relationships and surface characteristics

The cured LPU network coatings were evaluated to relate surface and mechanical characteristics to Xanthophyll-derived LPU network formation. All measurements were performed under controlled laboratory conditions, and reported values represent the average of at least three independent experiments. Surface gloss was measured at a 60° incident angle using a digital gloss meter (BYK Additives & Instruments, Germany) after calibration with a standard reference tile. Pencil hardness was assessed using a pencil hardness tester (BYK Additives & Instruments, Germany) in accordance with ASTM D3363, employing pencils ranging from 9B to 9H Impact resistance was evaluated using a falling weight impact tester with a 4.10 lb indenter dropped from heights of 5–100 cm, and the coatings were examined for cracking, peeling, or loss of adhesion to assess network integrity resulting from lutein transformation.

2.9. Chemical resistance and network integrity

The chemical resistance of the LPU coatings was evaluated in accordance with ASTM D543–67 (1972) to assess the integrity of the chemically transformed networks. Coated panels were immersed for seven days in acidic (1 N H_2SO_4 and 1 N HCl), alkaline (1 N NaOH), and organic solvent media. After exposure, the samples were air-dried for 1 h and visually examined for changes in appearance, gloss, or film continuity, providing qualitative insight into network stability arising from lutein transformation.

The resistance of the LPU networks to aggressive ionic environments was further examined by immersion in 3.5 wt% aqueous NaCl solution, a commonly used corrosive medium. Both intact and deliberately scribed coated steel panels were evaluated alongside uncoated steel substrates, with the scribe introduced using a sharp razor blade (10 μm). The panels were immersed for up to 144 h and extended to 192 h, with periodic visual inspection and photographic documentation used to monitor corrosion development and coating degradation, thereby assessing the protective integrity of the LPU networks.

2.10. Static water contact angle and surface free energy

Static water contact angle measurements of the LPU films were performed using a contact angle goniometer (e.g., Krüss DSA100, Germany) under ambient conditions by the sessile drop method, in which a ~5 μL droplet of deionized water was deposited on the film surface and the contact angle recorded after stabilization. Measurements were taken at multiple locations on each sample and averaged. Surface free energy was calculated from the contact angle data using the Young-Dupré approach, with polar and dispersive components determined using at least two probe liquids with known surface tension parameters (e.g., water and diiodomethane), allowing assessment of surface wettability changes resulting from the chemical transformation of lutein.

3. Results and discussion

3.1. Lutein extraction and purification

Lutein was successfully isolated from *Tagetes erecta* petals following the extraction and purification procedure described in Section 2.1.1. The extraction afforded bright yellow crystalline lutein with an overall isolated yield of 2.6–4.3% (w/w) based on the dry weight of marigold petals [26,27]. Following saponification and recrystallization, the purified lutein exhibited a characteristic absorption maximum at 445 nm, and UV–Vis analysis indicated a purity exceeding 94%, confirming the effective removal of chlorophylls, carotenoid esters, and other plant-derived impurities.

The high purity of the isolated lutein ensured the availability of two reactive terminal hydroxyl groups required for subsequent polyurethane synthesis. The purified lutein was readily soluble in DMAc and participated efficiently in the step-growth polyaddition reaction with aromatic diisocyanates, providing a suitable renewable xanthophyll precursor for the preparation of lutein-derived polyurethane (LPU) networks.

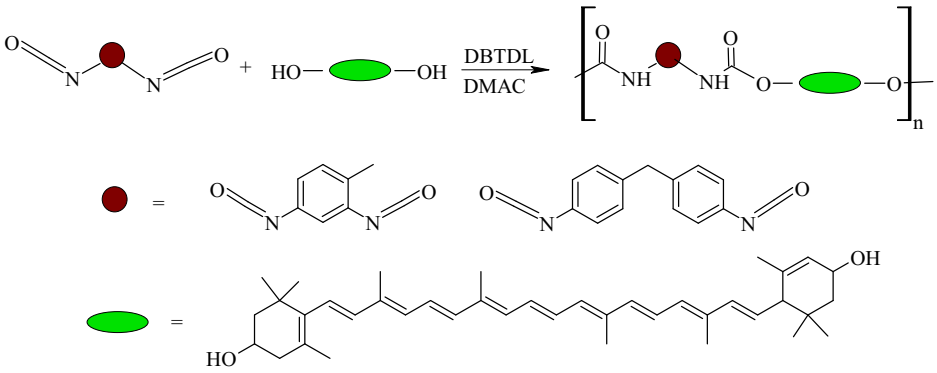

Scheme 1. Schematic representation of the Xanthophyll-derived step-growth polymerization of lutein into LPU networks.

3.2. Spectroscopic characterization of lutein

The FTIR and ^{1}H NMR spectra confirmed the structure of lutein and the presence of reactive hydroxyl functionalities. The FTIR spectrum exhibited a broad absorption band at 3389 cm^{-1} corresponding to O—H stretching vibrations, along with characteristic bands at 1651–1524 cm^{-1} attributed to the conjugated C=C bonds of the polyene backbone. The absorptions at 1267–1068 cm^{-1} were assigned to C—O stretching vibrations of the secondary alcohol groups [28]. In the ^{1}H -NMR spectrum, multiplets observed at δ 6.7–5.8 ppm were assigned to olefinic

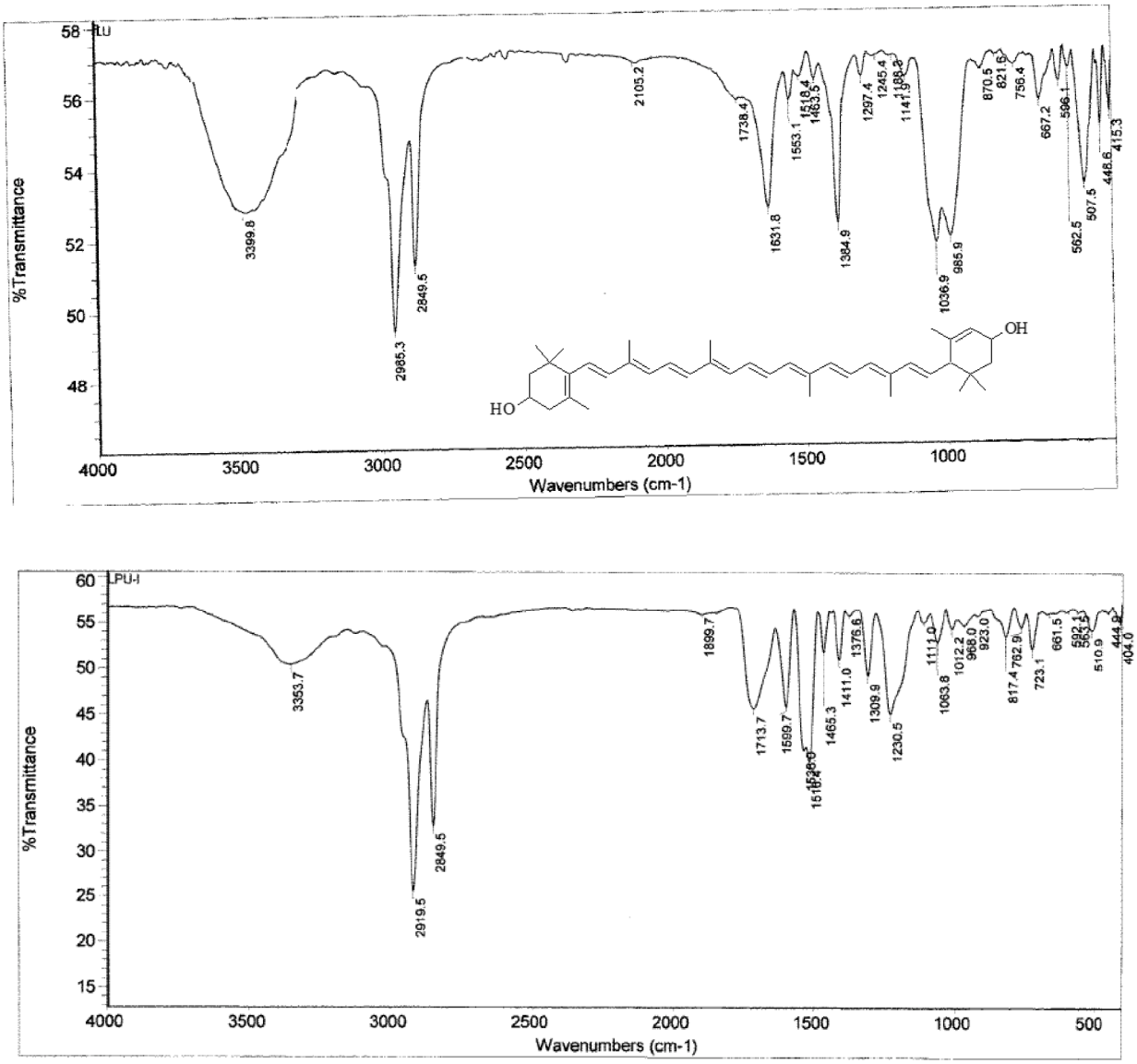

Fig. 1. FTIR spectra of a) lutein, b) LPU.

Table 1
Influence of NCO/OH molar ratio on molecular weight and intrinsic viscosity of LPU networks.

Sample	NCO/OH Molar Ratio	Mn[a] (g mol^{-1})	Mw[a] (g mol^{-1})	PDI	Intrinsic Viscosity[b] [η] (dL g^{-1})
LPU-1	0.5:1	19,236	42,364	2.20	0.22
	1.0: 1	24,726	68,772	2.78	0.24
	1.5: 1	17,254	26,823	1.55	0.18
	2.0:1	12,345	23,670	1.91	0.16
	2.5: 1	8632	13,456	1.57	0.10
	3.0: 1	5382	11,867	2.20	0.08
LPU-2	0.5:1	20,124	46,307	2.30	0.22
	1.0:1	24,186	67,286	2.78	0.24
	1.5:1	16,935	27,875	1.65	0.18
	2.0:1	13,695	24,521	1.79	0.16
	2.5:1	9223	14,849	1.61	0.11
	3.0:1	5786	12,468	2.15	0.09
LPU-3	0.5:1 (0.5:0.5)	17,695	43,568	2.46	0.22
	1.0:1 (0.5:0.5)	22,015	66,238	3.01	0.24
	1.5:1 (0.5:0.5)	17,510	23,658	1.35	0.16
	2.0:1 (0.5:0.5)	12,542	21,023	1.68	0.15
	2.5:1 (0.5:0.5)	11,253	17,546	1.56	0.13
	3.0:1 (0.5:0.5)	7562	11,245	1.49	0.09

[a]TDI = Toluene diisocyanate; [b]MDI = Methylene diphenyl diisocyanate; [c]TDI + MDI.

protons of the conjugated polyene chain, while broad signals at δ 3.97 and 3.83 ppm corresponded to the two hydroxyl protons. Resonances between δ 1.7 and 0.9 ppm were attributed to methyl groups attached to the polyene backbone and terminal ionone rings [28,29]. The mass spectrum exhibited a molecular ion peak consistent with the molecular weight of lutein, confirming its molecular composition. These spectral features are consistent with the reported structure of lutein and confirm the availability of hydroxyl groups for subsequent urethane formation during polyurethane synthesis [28,29]. These results establish the availability of reactive hydroxyl groups required for subsequent polyurethane formation.

3.3. Chemical transformation of lutein

The LPU were synthesized through step-growth polyaddition reactions between the hydroxyl functionalities of lutein and the isocyanate groups of aromatic diisocyanates, namely methylene diphenyl diisocyanate (MDI) and toluene diisocyanate (TDI), at varying NCO/OH molar ratios (Scheme 1). This work extends our previous investigations on curcumin-based segmented polyurethanes [30], wherein naturally occurring polyphenolic scaffolds were transformed into urethane-linked polymeric architectures. In the present study, lutein, a polyhydroxy xanthophyll carotenoid, serves as a bio-based synthon whose terminal hydroxyl groups undergo selective reaction with diisocyanates to form urethane linkages. The influence of diisocyanate structure and NCO/OH stoichiometry on chain growth, network development, molecular weight evolution, intrinsic viscosity, and coating performance was systematically examined. The results provide insight into the utilization of xanthophyll-derived molecular building blocks for the preparation of functional polyurethane materials.

FTIR spectroscopy confirms the conversion of lutein into LPU networks. Native lutein exhibits a characteristic broad -OH stretching band centered at 3427 cm^{-1}, arising from its phenolic and aliphatic hydroxyl groups. The complete disappearance of this band in the LPU spectra indicates effective consumption of lutein -OH functionalities during the polyurethane-forming reaction.

Simultaneously, new absorption bands emerge in the transformed materials, characteristic of urethane linkage formation. The broad band observed at 3353 cm^{-1} is assigned to urethane -NH stretching vibrations, while the strong band at 1713 cm^{-1} corresponds to C═O stretching of the urethane carbonyl group. In addition, the appearance of a prominent band at 1230 cm^{-1} is attributed to C—O-C stretching vibrations, further corroborating the formation of urethane bonds within the polymer network [31–33].

Importantly, the characteristic isocyanate absorption band in the range 2270–2250 cm^{-1}, present in the diisocyanate precursors (MDI and TDI), is completely absent in the LPU spectra. This confirms the complete consumption of reactive -NCO groups, indicating efficient polyaddition between lutein hydroxyl groups and diisocyanates [31]. Collectively, these spectral changes confirm the successful conversion of lutein into LPU networks. Fig. 1

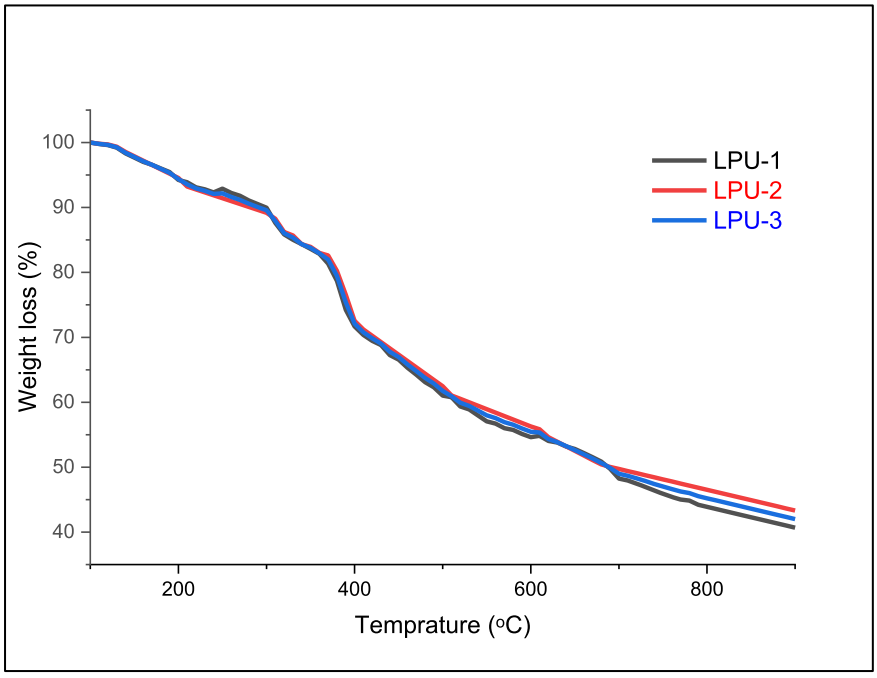

Fig. 2. Thermogravimetric analysis (TGA) curves of LPU networks.

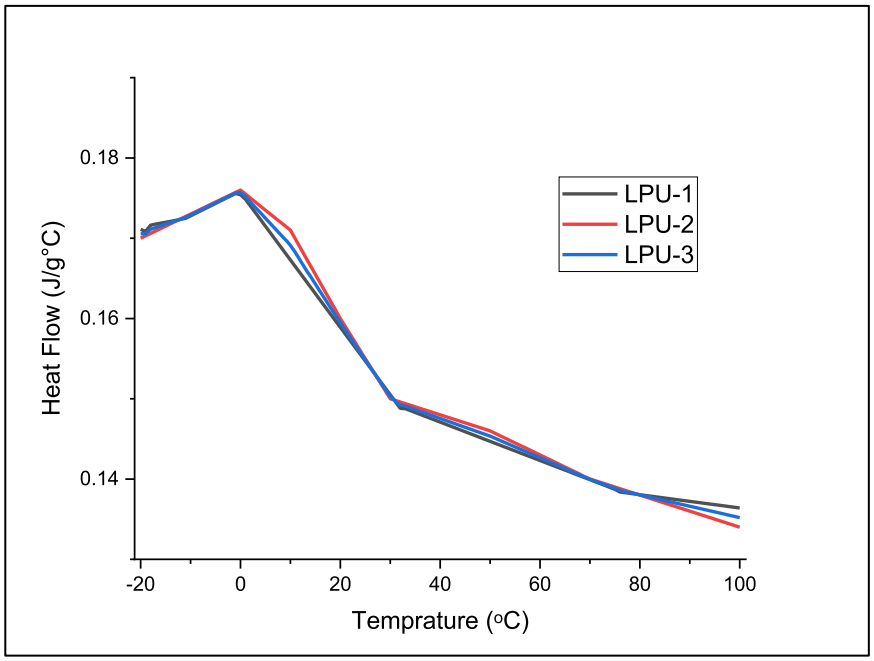

Fig. 3. DSC thermogram of LPU networks.

3.4. Molecular weight determination and intrinsic viscosity

The GPC results (Table 1) demonstrate the characteristic behavior of step-growth polymerization, where molecular weight reaches a maximum only at near-stoichiometric reactant ratios. Accordingly, all three LPU systems exhibited their highest molecular weights at an NCO/OH ratio of 1.0:1. LPU-1 showed the highest Mn and Mw values of 24,726 and 68,772 g mol^{-1}, respectively, followed by LPU-2 (24,186 and 67,286 g mol^{-1}) and LPU-3 (22,015 and 66,238 g mol^{-1}). These samples also displayed the highest intrinsic viscosity (0.24 dL g^{-1}), confirming efficient chain extension and the formation of longer polymer chains under balanced stoichiometric conditions [34,35].

At lower (0.5:1) or higher (1.5:1–3.0:1) NCO/OH ratios, both Mn and Mw decreased substantially, accompanied by a reduction in intrinsic viscosity to 0.08–0.18 dL g^{-1}. This behavior is consistent with step-growth polymerization, where any deviation from stoichiometric balance limits the probability of functional group coupling, resulting in premature chain termination and shorter polymer chains [34,35].

The highest polydispersity indices (PDI) were also observed at the 1.0:1 ratio, reaching 2.78 for LPU-1 and LPU-2 and 3.01 for LPU-3. Rather than indicating poor reaction control, these values reflect the heterogeneous nature of network formation during the later stages of step-growth polymerization. Lutein contains two structurally distinct secondary hydroxyl groups on the β- and ε-ionone rings, whose unequal steric accessibility and reactivity toward aromatic diisocyanates produce non-uniform chain extension and localized network formation [34,35]. The slightly higher PDI of LPU-3 suggests that the combined use of TDI and MDI introduces additional kinetic heterogeneity owing to their different isocyanate reactivities. Similar broad molecular weight distributions have been reported for other rigid phytochemical diols, including curcumin-based polyurethane systems, where structural asymmetry governs network evolution during step-growth polymerization [30,34,35].

Table 2
Effect of NCO/OH molar ratio on coating properties of LPU.

Sample	Diisocyanate system	NCO/OH molar ratio	Touch Dry Time[a] (h)	Gloss 60°	Pencil hardness	Impact Resistance [b,c]
LPU-1	**TDI**	0.5:1	10	78.6	1H	1.2 kg m
		1.0: 1	9	81.6	2H	1.5 kg m
		1.5: 1	9.5	74.5	1H	1.0 kg m
		2.0:1	8	75.2	1H	>0.5 kg m
		2.5: 1	6	68.4	1H	>0.5 kg m
		3.0: 1	4	62.9	1H	>0.5 kg m
LPU-2	**MDI**	0.5:1	11	77.3	1H	1.0 kg m
		1.0:1	9.5	82.4	2H	1.2 kg m
		1.5:1	8.2	75.9	1H	0.8 kg m
		2.0:1	7	75.1	1H	>0.5 kg m
		2.5:1	6	66.3	1H	>0.5 kg m
		3.0:1	5.5	64.5	1H	>0.5 kg m
LPU-3	TDI + MDI	0.5:1 (0.5:0.5)	9.5	78.8	1H	1.2 kg m
		1.0:1 (0.5:0.5)	8	80.9	2H	1.4 kg m
		1.5:1 (0.5:0.5)	7	76.4	1H	0.9 kg m
		2.0:1 (0.5:0.5)	6	73.6	1H	>0.5 kg m
		2.5:1 (0.5:0.5)	5	70.3	1H	>0.5 kg m
		3.0:1 (0.5:0.5)	3	68.6	1H	>0.5 kg m

[a] Touch Dry time in hours; [b]Direct Impact Resistance; [c]Reverse Impact resistance.

Table 3
Qualitative chemical resistance of LPU networks in organic solvents and corrosive media.

Sample	Diisocyanate system	NCO/OH molar ratio	Acetone	DMSO	DMAC	NMP	THF	1 N H_2SO_4	1 N HCl	1 N NaOH
LPU-1	TDI	0.5:1	-	-	-	-	-	-	-	-
		1.0:1	#	#	#	#	#	-	-	-
		1.5:1	#	#	#	#	#	-	-	-
		2.0:1	#	#	#	#	#	-	-	-
		2.5:1	#	#	#	#	#	-	-	-
		3.0:1	-	-	-	-	-	-	-	-
LPU-2	MDI	0.5:1	-	-	-	-	-	-	-	-
		1.0:1	#	#	#	#	#	-	-	-
		1.5:1	#	#	#	#	#	-	-	-
		2.0:1	#	#	#	#	#	-	-	-
		2.5:1	#	#	#	#	#	-	-	-
		3.0:1	-	-	-	-	-	-	-	-
LPU-3	TDI + MDI	0.5:1 (0.5:0.5)	-	-	-	-	-	-	-	-
		1.0:1 (0.5:0.5)	#	#	#	#	#	-	-	-
		1.5:1 (0.5:0.5)	#	#	#	#	#	-	-	-
		2.0:1 (0.5:0.5)	#	#	#	#	#	-	-	-
		2.5:1 (0.5:0.5)	#	#	#	#	#	-	-	-
		3.0:1 (0.5:0.5)	-	-	-	-	-	-	-	-

Note: '+' soluble, '–' insoluble, '#' swelling.

3.5. Thermal behavior of LPU networks

The thermogravimetric analysis (Fig. 2) revealed that the LPU networks possess good thermal stability, with negligible mass loss below approximately 250 °C, primarily due to the removal of residual solvent or absorbed moisture. All formulations exhibited a two-step degradation profile. The first degradation stage is attributed to the cleavage of urethane linkages, while the second corresponds to decomposition of the lutein-derived xanthophyll backbone. Approximately 60% mass loss was observed up to 550 °C, after which further degradation was minimal, indicating the formation of a thermally stable char residue [36]. The enhanced thermal stability correlates well with the higher molecular weights and improved network integrity obtained at the optimum NCO/OH ratio (1.0:1), confirming efficient chain extension during polyurethane formation. This improved network integrity also correlates with the superior mechanical properties observed for these formulations, including higher coating hardness and impact resistance.

The DSC thermogram (Fig. 3) exhibited a glass transition temperature (Tg) of 21.46 °C without a distinct melting endotherm, confirming the predominantly amorphous nature of the LPU networks. The low enthalpy change ($\Delta H = 0.03586\ J\ g^{-1}{}^{\circ}C^{-1}$) indicates restricted segmental mobility resulting from urethane bond formation and physical network interactions. The absence of crystalline domains is consistent with the broad molecular weight distribution obtained from GPC, where the asymmetric structure of lutein and heterogeneous step-growth polymerization hinder regular chain packing. This amorphous morphology contributes to the balanced combination of flexibility, thermal stability, and mechanical performance exhibited by the LPU coatings [37].

3.6. Structure–Property relationships and surface characteristics

The influence of functional group (NCO/OH) stoichiometry on the surface and mechanical characteristics of the LPU networks is summarized in Table 2. Variations in the NCO/OH molar ratio directly affect the extent of lutein transformation, molecular organization, and network density, thereby governing the observed structure-property relationships.

Near-equimolar compositions (NCO/OH = 1.0:1.0) consistently exhibited the highest gloss values (80–82), maximum pencil hardness (2H), and superior impact resistance across all diisocyanate systems. These trends can be attributed to efficient chemical transformation of lutein hydroxyl groups under near-stoichiometric conditions, which favors optimal chain extension and network formation, as supported by the higher molecular weight and improved network architecture obtained under near-stoichiometric conditions.

Table 4
Quantitative swelling ratio and chemical stability of LPU networks after 7-day immersion.

Sample	Diisocyanate System	Stoichiometry (NCO/OH)	Swelling Ratio in THF ('Qm %')	Mass Loss in 1 N HCl ('WL %')	Mass Loss in 1 N NaOH ('WL %')
LPU-1	TDI	0.5:1.0	Dissolved / Disintegrated	4.2 ± 0.3	5.8 ± 0.4
		1.0:1.0	18.4 ± 1.2	0.3 ± 0.05	0.6 ± 0.09
		2.0:1.0	12.1 ± 0.9	0.1 ± 0.02	0.2 ± 0.04
LPU-2	MDI	0.5:1.0	17.2 ± 1.0	0.6 ± 0.03	0.8 ± 0.04
		1.0:1.0	14.2 ± 1.1	0.2 ± 0.04	0.4 ± 0.07
		2.0:1.0	13.1 ± 1.2	0.7 ± 0.08	0.3 ± 0.02
LPU-3	TDI + MDI	1.0:1.0	16.1 ± 1.3	0.2 ± 0.03	0.5 ± 0.08

At higher NCO/OH ratios, a progressive reduction in gloss and mechanical performance was observed, despite shorter drying times. Excess isocyanate limits effective chain growth, leading to lower molecular weights and reduced hydrodynamic volume, which in turn diminishes cohesive strength within the LPU network [33,37]. The faster drying behavior at elevated NCO/OH ratios reflects increased isocyanate reactivity rather than enhanced network integrity.

These results demonstrate that the macroscopic surface and mechanical characteristics of the coatings are governed by the extent and efficiency of lutein transformation, highlighting how NCO/OH stoichiometry controls network architecture and emergent material properties [37].

3.7. Chemical resistance and network integrity

The chemical resistance and network integrity of the LPU networks were evaluated by qualitative solvent resistance (Table 3) and quantitative swelling and gravimetric mass-loss measurements (Table 4). All formulations were insoluble in 1 N H_2SO_4, 1 N HCl, and 1 N NaOH, confirming the formation of chemically stable urethane linkages through successful transformation of the lutein hydroxyl groups [39]. In

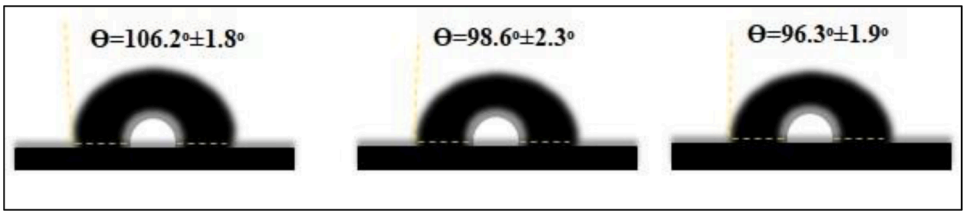

Fig. 4. Static water contact angle images of LPU networks.

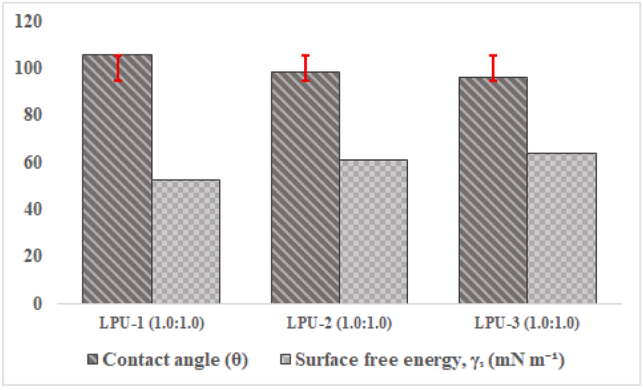

Fig. 5. Apparent surface free energy of LPU networks.

polar aprotic solvents (acetone, DMSO, DMAc, NMP, and THF), the near-stoichiometric formulations (1.0:1.0–2.5:1.0) exhibited controlled swelling without dissolution, indicating the formation of continuous, highly associated LPU networks [40].

The quantitative data (Table 4) showed low swelling ratios (12.1–18.4%) and negligible mass loss (<1%) for the near-stoichiometric networks after 7 days of immersion, whereas the LPU-1 sample prepared at an NCO/OH ratio of 0.5:1.0 dissolved in THF and exhibited higher mass losses (4.2–5.8%), indicating an incompletely developed network [41]. These results correlate well with the GPC analysis, where the highest **Mn, Mw**, and intrinsic viscosity were obtained at the 1.0:1.0 ratio, confirming efficient step-growth polymerization and the formation of longer polymer chains with greater network integrity [42].

These observations agree well with the GPC, thermal, and coating performance results, confirming that the near-stoichiometric formulations develop the most robust LPU networks through efficient step-growth polymerization.

3.8. Static water contact angle and surface free energy

Static water contact angle measurements were employed to probe the influence of lutein incorporation on the surface characteristics of the resulting urethane networks. Representative contact angle images of LPU films are shown in Fig. 4. LPU-1, LPU-2, and LPU-3 prepared at an NCO/OH molar ratio of 1.0:1.0 exhibited contact angles of 106.2 ± 1.8°, 98.6 ± 2.3°, and 96.3 ± 1.9°, respectively, indicating predominantly hydrophobic surfaces [38]. The observed hydrophobicity can be attributed to the rigid polyene backbone of the xanthophyll moiety and the effective consumption of polar hydroxyl groups during urethane formation.

Apparent surface free energy values calculated using the Young–Dupré equation (Fig. 5) increased from 52.6 mN m^{-1} for LPU-1 to 64.1 mN m^{-1} for LPU-3, reflecting systematic modulation of surface energetics arising from variations in diisocyanate composition and phytochemical integration. These results demonstrate that chemical transformation of lutein not only governs bulk molecular organization but also enables tunable surface wettability, highlighting the role of xanthophyll-derived structures in controlling interfacial properties. The improved hydrophobicity is also consistent with the excellent chemical resistance of the LPU networks, as reduced water affinity limits solvent penetration and enhances long-term durability.

4. Conclusion

This study demonstrates that lutein can serve as an effective renewable bifunctional xanthophyll synthon for polyurethane synthesis through step-growth polymerization with aromatic diisocyanates. Near-stoichiometric formulations produced the highest molecular weights, improved network integrity, superior thermal stability, enhanced coating performance, and excellent resistance toward acidic, alkaline, and solvent environments. The strong correlation between molecular architecture, thermal behavior, mechanical properties, and chemical durability confirms that the LPU networks possess characteristics comparable to conventional polyurethane coatings. These findings highlight the potential of naturally occurring xanthophylls as sustainable building blocks for advanced coating and polymer applications. Overall, the present work demonstrates that naturally occurring xanthophylls can serve as sustainable molecular building blocks for developing high-performance bio-based polyurethane coatings.

CRediT authorship contribution statement

Rahul D. Kamble: Writing – original draft, Supervision, Methodology, Investigation, Formal analysis, Conceptualization. **Shrikant V. Hese:** Writing – review & editing, Validation, Formal analysis, Data curation. **Ajay N. Ambhore:** Writing – review & editing, Methodology, Formal analysis, Data curation. **Milind V. Gaikwad:** Writing – review & editing, Visualization, Methodology, Formal analysis. **Shudhodan N. Kadam:** Writing – review & editing, Software, Investigation, Formal analysis.

Declaration of interests

The authors declare that they have no known competing financial interests or personal relationships that could have appeared to influence the work reported in this paper.

Acknowledgements

The authors sincerely acknowledge Amruteshwar College, Vinzar, for providing laboratory facilities and continuous institutional support.

Supplementary materials

Supplementary material associated with this article can be found, in the online version, at doi:10.1016/j.nexres.2026.102174.

References

[1] M. Pu, C. Fang, X. Zhou, D. Wang, Y. Lin, W. Lei, L. Li, Recent advances in environment-friendly polyurethanes from polyols recovered from the recycling and renewable resources: a review, Polymers 16 (13) (2024) 1889, https://doi.org/10.3390/polym16131889.

[2] E. Delebecq, J. Pascault, B. Boutevin, F. Ganachaud, On the versatility of urethane/urea bonds: reversibility, blocked isocyanate, and non-isocyanate polyurethane, Chem. Rev. 113 (1) (2013) 80–118, https://doi.org/10.1021/cr300195n.

[3] E. Balla, D.N. Bikiaris, N. Pardalis, N.D. Bikiaris, Toward sustainable polyurethane Alternatives: a review of the synthesis, applications, and lifecycle of non-isocyanate polyurethanes (NIPUs), Polymers 17 (10) (2025) 1364, https://doi.org/10.3390/polym17101364.

[4] Y. Li, X. Luo, S. Hu, Polyols and polyurethanes from vegetable oils and their derivatives. Springer Briefs in Molecular Science, 2015, pp. 15–43, https://doi.org/10.1007/978-3-319-21539-6_2.

[5] Ż. Ciastowicz, R. Pamuła, A. Białowiec, Utilization of plant oils for sustainable polyurethane adhesives: a review, Material 17 (8) (2024) 1738, https://doi.org/10.3390/ma17081738.

[6] T.H. Kim, H.S. Kim, S. Lee, Sustainable polyurethane systems: integrating green synthesis and closed-loop recovery, Polymers 18 (2) (2026) 246, https://doi.org/10.3390/polym18020246.

[7] H. Feng, Y. Wang, T. Zhang, J. Wang, Z. Jia, S. Jiang, X. Han, Review on research progress on bio-based self-healing polyurethane, ACS Mater. Lett. 7 (10) (2025) 3461–3488, https://doi.org/10.1021/acsmaterialslett.5c01153.

[8] P.T. Anastas, Theor. Pract. (1998).

[9] S.A. Gunbatar, B.E. Kiran, Y. Boz, E.S. Oztay, A systematic review of green and sustainable chemistry training research with pedagogical content knowledge framework: current trends and future directions, Chem. Educ. Res. Pract. 26 (1) (2024) 34–52, https://doi.org/10.1039/d4rp00166d.

[10] O. Akay, C. Altinkok, G. Acik, H. Yuce, G.K. Ege, A bio-based and non-toxic polyurethane film derived from Luffa cylindrica cellulose and L-lysine diisocyanate ethyl ester, Eur. Polym. J. 161 (2021) 110856, https://doi.org/10.1016/j.eurpolymj.2021.110856.

[11] B. Acik, G. Acik, H. Erdemi, Synthesis and characterization of bile acid, poly (ε-caprolactone) and L-lysine diisocyanate ethyl ester based polyurethanes and investigation of their biodegradability properties, Eur. Polym. J. 146 (2021) 110247, https://doi.org/10.1016/j.eurpolymj.2020.110247.

[12] M. Cappello, S. Filippi, D. Rossi, P. Cinelli, I. Anguillesi, C. Camodeca, E. Orlandini, G. Polacco, M. Seggiani, Waste-cooking-oil-derived polyols to produce new sustainable rigid polyurethane foams, Sustainability 16 (21) (2024) 9456, https://doi.org/10.3390/su16219456.

[13] Y. Mo, X. Huang, C. Hu, Recent advances in the preparation and application of Bio-based polyurethanes, Polymers 16 (15) (2024) 2155, https://doi.org/10.3390/polym16152155.

[14] J.M. Lang, U.M. Shrestha, M. Dadmun, The effect of plant source on the properties of Lignin-based polyurethanes, Front. Energy Res. 6 (2018), https://doi.org/10.3389/fenrg.2018.00004.

[15] F.R. Vieira, S. Magina, D.V. Evtuguin, A. Barros-Timmons, Lignin as a renewable building block for sustainable polyurethanes, Materials 15 (17) (2022) 6182, https://doi.org/10.3390/ma15176182.

[16] J.D. Bhaliya, S.N.R. Kutcherlapati, N. Dhore, N. Punugupati, K.L. Sunkara, S. Misra, S.S.K. Joshi, Soybean oil-derived, non-isocyanate polyurethane–TiO 2 nanocomposites with enhanced thermal, mechanical, hydrophobic and antimicrobial properties, RSC Sustain. 3 (3) (2025) 1434–1447, https://doi.org/10.1039/d4su00587b.

[17] M. Rayung, N.A. Ghani, N. Hasanudin, A review on vegetable oil-based non isocyanate polyurethane: towards a greener and sustainable production route, RSC Adv 14 (13) (2024) 9273–9299, https://doi.org/10.1039/d3ra08684d.

[18] Z. Li, Z. Du, Y. Wang, Y. Feng, R. Zhang, X. Yan, Chemical modification, characterization, and activity changes of land plant polysaccharides: a review, Polymers 14 (19) (2022) 4161, https://doi.org/10.3390/polym14194161.

[19] R.C. O'Halloran, A.J. Shapiro, Y. Gupta, A. Long, S.G. Haney, Y. Otsuka, S. Sadula, D.G. Vlachos, D.F. Levia, T.H. Epps, Following forest cues for the harvest optimization of tomorrow's biofeedstocks, Green Chem. 28 (2025) 827–838, https://doi.org/10.1039/d5gc04279h.

[20] E. Rodríguez-deLeón, M. Bah, J.O.C. Jiménez-Halla, J. Bonilla-Cruz, M. Estévez, J. E. Báez, Synthesis and characterization of segmented poly(ester-urethane)s (PEUs) containing carotenoids, Polym. Chem. 10 (48) (2019) 6580–6587, https://doi.org/10.1039/c9py01487j.

[21] C. Molteni, C. La Motta, F. Valoppi, Improving the bioaccessibility and bioavailability of carotenoids by means of nanostructured delivery systems: a comprehensive review, Antioxidants 11 (10) (2022) 1931, https://doi.org/10.3390/antiox11101931.

[22] S. Pongcharoen, P. Warnnissorn, O. Lertkajornsin, N. Limpeanchob, M. Sutheerawattananonda, Protective effect of silk lutein on ultraviolet B-irradiated human keratinocytes, Biol. Res. 46 (1) (2013) 39–45, https://doi.org/10.4067/s0716-97602013000100006.

[23] W. Zhang, Y. Zhao, Z. Shi, D. Cong, Y. Bai, Lutein inhibits cell growth and activates apoptosis via the PI3K/AKT/MTOR signaling pathway in a549 human Non-small-cell lung cancer cells, J. Environ. Pathol. Toxicol. Oncol. 37 (4) (2018) 341–350, https://doi.org/10.1615/jenvironpatholtoxicoloncol.2018027418.

[24] D.B. Rodriguez-Amaya, P. Esquivel, A.J. Meléndez-Martínez, Comprehensive update on carotenoid colorants from plants and microalgae: challenges and advances from research laboratories to industry, Foods 12 (22) (2023) 4080, https://doi.org/10.3390/foods12224080.

[25] A. Uva, A. Lin, H. Tran, Biobased, degradable, and conjugated poly(Azomethine)s, J. Am. Chem. Soc. 145 (6) (2023) 3606–3614, https://doi.org/10.1021/jacs.2c12668.

[26] S. Manzoor, R. Rashid, B.P. Panda, V. Sharma, M. Azhar, Green extraction of lutein from marigold flower petals, process optimization and its potential to improve the oxidative stability of sunflower oil, Ultrason. Sonochem. 85 (2022) 105994, https://doi.org/10.1016/j.ultsonch.2022.105994.

[27] R. Kumar, W. Yu, C. Jiang, C. Shi, Y. Zhao, Improvement of the isolation and purification of lutein from marigold flower (tagetes erecta l.) and its antioxidant activity, J. Food Process Eng. 33 (6) (2010) 1065–1078, https://doi.org/10.1111/j.1745-4530.2008.00326.x.

[28] Q. Zhang, J. Wang, C. Li, M. Zheng, Z. He, Y. Zou, H. Xiong, B. Xu, W. Xiang, J. Tang, Characterization and bioactive potential of carotenoid lutein from Gordonia rubripertncta GH-1 isolated from traditional Pixian Douban, Foods 11 (22) (2022) 3649, https://doi.org/10.3390/foods11223649.

[29] E. Rodríguez-deLeón, M. Bah, J.E. Báez, M.T. Hernández-Sierra, K.J. Moreno, A. Nuñez-Vilchis, J. Bonilla-Cruz, K.J. Shea, Sustainable xanthophylls-containing poly(ε-caprolactone)s: synthesis, characterization, and use in green lubricants, RSC Adv. 12 (48) (2022) 30851–30859, https://doi.org/10.1039/d2ra04502h.

[30] R.D. Kamble, S.V. Hese, M.V. Gaikwad, Curcumin-based polyurethane coatings: a novel bioactive solution, J. Chem. Appl. (2024) 1–5, https://doi.org/10.47363/jcia/2024(3)136.

[31] J. Li, S. Jiang, L. Ding, L. Wang, Reaction kinetics and properties of MDI base poly (urethane-isocyanurate) network polymers, Des. Monomer. Polym. 24 (1) (2021) 265–273, https://doi.org/10.1080/15685551.2021.1971858.

[32] C.K. Patil, D.W. Jung, H.D. Jirimali, J.H. Baik, V.V. Gite, S.C. Hong, Nonedible vegetable oil-based polyols in anticorrosive and antimicrobial polyurethane coatings, Polymers 13 (18) (2021) 3149, https://doi.org/10.3390/polym13183149.

[33] A.M. Patil, H.D. Jirimali, V.V. Gite, R.N. Jagtap, Synthesis and performance of bio-based hyperbranched polyol in polyurethane coatings, Prog. Org. Coat. 149 (2020) 105895, https://doi.org/10.1016/j.porgcoat.2020.105895.

[34] N. Amjed, I.A. Bhatti, K.M. Zia, J. Iqbal, Y. Jamil, Synthesis and characterization of stable and biological active chitin-based polyurethane elastomers, Int. J. Biol. Macromol. 154 (2020) 1149–1157, https://doi.org/10.1016/j.ijbiomac.2019.11.097.

[35] F. Colucci, V. Mancini, C. Mattu, M. Boffito, Designing multifunctional devices for regenerative pharmacology based on 3D scaffolds, drug-loaded nanoparticles, and thermosensitive hydrogels: a proof-of-concept study, Pharmaceutics 13 (4) (2021) 464, https://doi.org/10.3390/pharmaceutics13040464.

[36] N.T. Dintcheva, G. Infurna, M. Baiamonte, F. D'Anna, Natural compounds as sustainable additives for biopolymers, Polymers 12 (4) (2020) 732, https://doi.org/10.3390/polym12040732.

[37] D. Chattopadhyay, K. Raju, Structural engineering of polyurethane coatings for high performance applications, Prog. Polym. Sci. 32 (3) (2007) 352–418, https://doi.org/10.1016/j.progpolymsci.2006.05.003.

[38] M.S. De Luna, Recent trends in waterborne and Bio-based polyurethane coatings for corrosion protection, Adv Mater Interfac. 9 (11) (2022), https://doi.org/10.1002/admi.202101775.

[39] N. Mumtaz, N. Akram, K.M. Zia, M. Saeed, M. Usman, Fabrication, Thermo-mechanical, and morphological characterization of hydroxyapatite-reinforced polyurethane biocomposites as dye adsorbent for effluent, ACS Omeg. 8 (37) (2023) 33310–33320, https://doi.org/10.1021/acsomega.3c02371.

[40] S. Gopalakrishnan, T.L. Fernando, Influence of polyols on properties of bio-based polyurethanes, Bull. Mater. Sci. 35 (2) (2012) 243–251, https://doi.org/10.1007/s12034-012-0279-5.

[41] I. Palle, V. Lodin, A.A.M. Yunus, S.H. Lee, P.M. Tahir, N. Hori, P. Antov, A. Takemura, Effects of NCO/OH ratios on bio-based polyurethane film properties made from Acacia mangium liquefied wood, Polymers 15 (5) (2023) 1154, https://doi.org/10.3390/polym15051154.

[42] L.D. Villar, T. Cicaglioni, M.F. Diniz, M.F.K. Takahashi, L.C. Rezende, Thermal aging of HTPB/IPDI-based polyurethane as a function of NCO/OH ratio, Mater. Res. 14 (3) (2011) 372–375, https://doi.org/10.1590/s1516-14392011005000063.